

LINEAR AND NONLINEAR REFRACTIVE INDEX CHANGES IN SPHERICAL QUANTUM DOT

B. Çakır^{1,*}, Y. Yakar², and A. Özmen¹

¹Physics Department, Faculty of Science, Selcuk University, Campus 42075, Konya, Turkey

²Physics Department, Faculty of Science and Letters, Aksaray University, Campus 68100, Aksaray, Turkey

Abstract—In this study, refractive index changes associated with intersubband transitions in a spherical quantum dot, GaAs/Al_xGa_{1-x}As, have been theoretically calculated in the presence of impurity. In this regard, the effect of dot radius, stoichiometric ratio, impurity and incident optical intensity on the refractive index changes have been investigated for the transitions between higher energy states, i.e., 1s-1p, 1p-1d and 1d-1f. The results show that these parameters have a great influence on the refractive index changes.

1. INTRODUCTION

Recent developments in modern technology have given an opportunity to confine the electrons in semiconductor nanostructures. The nanostructures with three-dimensional confinement of electrons are called Quantum Dots (QDs). QDs have found various application areas especially microelectronic and optoelectronic devices. These structures also exhibit the atomic properties like shell structures and discrete energy levels [1, 2]. Therefore, the electronic structures, energy states, optical and other physical properties of QDs with one- and two-electrons have been commonly studied by using various calculation methods [3–12]. The nonlinear optical properties of QD have the potential for device application such as infrared photo detectors, quantum dot lasers, high-speed electro-optical modulators, light emitting diodes, one electron transistors, optical memory technology and other extensive applications in optic communication. Therefore, in recently, the nonlinear properties of QD have attracted much

Received 9 August 2011, Accepted 26 September 2011, Scheduled 2 October 2011

* Corresponding author: Bekir Çakır (bcakir@selcuk.edu.tr).

attention for both practical applications and theoretical researches [13–34]. Ahn and Chuang [13] calculated the linear and nonlinear optical intersubband absorption coefficients for general asymmetric quantum well systems using the density matrix formalism. The optical absorption coefficients for the transitions between the ground and higher electronic energy states were investigated by some authors [17–20] using an approach which is a combination of Quantum Genetic Algorithm (QGA) procedure and Hartree-Fock Roothaan (HFR) method. Chen et al. [21] discussed the influences of an external electric field and incident optical intensity on the linear and nonlinear optical absorption coefficients in an asymmetric double triangular quantum wells. Şahin [24, 25] carried out the optical properties of a spherical QD using matrix diagonalization technique for a finite confining potential well model. Shao et al. [27] studied the third-harmonic generation coefficient for cylinder quantum dots under the influence of an applied electric field using the compact density-matrix approach and iterative method. Later, optical absorption coefficients and refractive index changes associated with intersubband transitions were calculated by Rezaei et al. [28, 30] in a two-dimensional QD system under the influence of a uniform magnetic field. Zhang et al. [31] examined the optical absorption coefficients and the changes in the refractive index in GaAs/AlGaAs parabolic quantum dots under the influence of an applied electric and magnetic fields by using a compact density matrix approach. In very recently, Kirak et al. [34] investigated in detail the influence of an external electric field of the electronic properties in a spherical quantum dot of parabolic confinement. Also, they studied the linear and the third-order nonlinear optical absorption coefficients and refractive index changes for the 1s-1p and 1p-1d transitions by using a variational procedure. All of the above mentioned studies, except [34], are concentrated on the calculation of the absorption coefficients and refractive index changes for the transition between the lowest energy states, which is the transition 1s-1p between the ground ($\ell = 0$) and the first excited ($\ell = 1$) state. Therefore, studies in this field are still important for both theoretical research and practical applications. To our knowledge, up to now the refractive index changes have not been investigated for the transitions between higher energy states, i.e., the 1p-1d and 1d-1f transitions of QD with and without impurity.

In the previous study [20], we computed the linear, the third-order nonlinear and the total absorption coefficients of a spherical QD with and without impurity. In the present study, we have calculated the linear, nonlinear and total refractive index (RI) changes of the spherical QD, GaAs/Al_xGa_{1-x}As, with and without impurity for the transitions 1s-1p, 1p-1d and 1d-1f.

2. THEORY

We consider a shallow hydrogenic impurity located at the center of a spherical QD confined by a finite spherical potential well with radius R . The Hamiltonian of this system can be written, in atomic units (au) and the effective mass approximation, as follows

$$H = -\frac{\nabla^2}{2m^*} - \frac{Z}{\varepsilon_r r} + V(r), \quad (1)$$

where Z is impurity charge, r is the distance between electron and impurity, m^* is the effective mass of electron and ε_r denotes the real part of relative electric permittivity of the medium. The confinement potential is assumed in a form of the spherical potential well, i.e., $V(r) = 0$ for $r < R$ and $V(r) = V_0$ for $r \geq R$. Time independent Schrödinger equation is given by

$$H\psi_i = E_i\psi_i, \quad (2)$$

in which E_i and ψ_i are the energies and wavefunctions of the system. The energies E_i and the wavefunctions ψ_i have been calculated by using the method that is a combination of the QGA and HFR given details in Refs. [5, 6].

In the electric dipole approximation, if the polarization of an electromagnetic radiation is chosen in z -direction, the dipole transition matrix element between i th state (lower) and f th state (upper) is given by

$$\langle M_z \rangle_{fi} = e \left\{ \int_0^R (\psi_f^{r < R})^* r \cos \theta \psi_i^{r < R} d\tau + \int_R^\infty (\psi_f^{r > R})^* r \cos \theta \psi_i^{r > R} d\tau \right\}, \quad (3)$$

where ψ_f ve ψ_i are the wavefunctions of upper and lower states. The wavefunctions within (outside) of QD have been labeled with $\psi^{r < R}$ ($\psi^{r > R}$).

The matrix element is important for calculation of different optical properties of a system related to electronic transitions. Dipole transitions in a spherical QD are allowed only between states satisfying the selection rules $\Delta\ell = \pm 1$, where ℓ is the angular momentum quantum number.

In order to calculate the RI changes we consider the interaction between the linearly polarized electromagnetic wave (angular frequency is ω) and QDs. If the wave length of the progressive electromagnetic wave is larger than dimension of a QD (10^3 \AA for UV visible), the amplitude of electromagnetic wave may be considered as a constant

throughout QD. Then the electric field of an incident wave can be expressed as

$$\tilde{E}(t) = 2\tilde{E}_0 \cos(\omega t) = \tilde{E}_0 (e^{i\omega t} + e^{-i\omega t}). \quad (4)$$

The electronic polarization $P(t)$ caused by the incident field $\tilde{E}(t)$ is defined as follows

$$P(t) = \varepsilon_0 \chi^{(1)}(\omega) \tilde{E}_0 e^{i\omega t} + \varepsilon_0 \chi^{(2)}(2\omega) \tilde{E}_0^2 e^{2i\omega t} + \varepsilon_0 \chi^{(3)}(3\omega) \tilde{E}_0^3 e^{3i\omega t} + c.c., \quad (5)$$

where the terms up to the third-order in \tilde{E} are retained. The terms $\chi^{(1)}(\omega)$, $\chi^{(2)}(2\omega)$ and $\chi^{(3)}(3\omega)$ are known as the linear, the second- and the third-order nonlinear optical susceptibilities, respectively, and ε_0 is the electrical permittivity of vacuum. In this study, it was not considered $\chi^{(2)}(2\omega)$ since the system has a spherical symmetry. The second-order nonlinear susceptibility can occur only in noncentrosymmetric structures, that is, in structures that do not display inversion symmetry [35].

The analytical expressions of the linear $\varepsilon_0 \chi^{(1)}(\omega)$ and the third-order nonlinear $\varepsilon_0 \chi^{(3)}(\omega)$ terms for a two-level quantum system are obtained as follows [16, 21, 25, 29]

$$\varepsilon_0 \chi^{(1)}(\omega) = \frac{\rho \left| \langle M \rangle_{fi} \right|^2}{E_{fi} - \hbar\omega - i\hbar\Gamma_0}, \quad (6)$$

and

$$\varepsilon_0 \chi^{(3)}(\omega) = - \frac{\rho \left| \langle M \rangle_{fi} \right|^2 \left| \tilde{E} \right|^2}{E_{fi} - \hbar\omega - i\hbar\Gamma_0} \times \left[\frac{4 \left| \langle M \rangle_{fi} \right|^2}{(E_{fi} - \hbar\omega)^2 + (\hbar\Gamma_0)^2} - \frac{\left(\langle M \rangle_{ff} - \langle M \rangle_{ii} \right)^2}{(E_{fi} - i\hbar\Gamma_0)(E_{fi} - \hbar\omega - i\hbar\Gamma_0)} \right], \quad (7)$$

in which ρ is electron charge density in QD, $E_{fi} = E_f - E_i$ denotes energy difference between i and f electronic states, $\hbar\omega$ is incident photon energy and $\Gamma_0 = 1/\tau$ is relaxation ratio for the states i and f . It should be noted that for more realistic calculations, the electron density is $\rho = n/V_{\text{QD}}$, n is the number of electrons in QD and V_{QD} is the volume of QD [25].

The susceptibility is related to the change in refractive index as follows [14, 15, 25]:

$$\frac{\Delta n}{n_r} = \text{Re} \left(\frac{\chi(\omega)}{2n_r^2} \right). \quad (8)$$

Using this relation, the analytical expressions for the linear and nonlinear refractive index changes are defined for a spherical symmetric systems [14, 15, 25]:

$$\frac{\Delta n^{(1)}(\omega)}{n_r} = \frac{\rho}{2n_r^2 \varepsilon_0} \left| \langle M \rangle_{fi} \right|^2 \left(\frac{E_f - E_i - \hbar\omega}{(E_f - E_i - \hbar\omega)^2 + (\hbar\Gamma_0)^2} \right), \quad (9)$$

and

$$\frac{\Delta n^{(3)}(\omega, I)}{n_r} = -\frac{\rho I \mu c}{n_r^3 \varepsilon_0} \left| \langle M \rangle_{fi} \right|^4 \left(\frac{E_f - E_i - \hbar\omega}{\left[(E_f - E_i - \hbar\omega)^2 + (\hbar\Gamma_0)^2 \right]^2} \right). \quad (10)$$

where μ is the permeability of the system defined as $\mu = 1/\varepsilon_0 c^2$, c is the speed of light in vacuum, $n_r = \sqrt{\varepsilon_r}$ represents the RI of semiconductor.

The total refractive index changes are given as

$$\frac{\Delta n(\omega, I)}{n_r} = \frac{\Delta n^{(1)}(\omega)}{n_r} + \frac{\Delta n^{(3)}(\omega, I)}{n_r}, \quad (11)$$

where the term I is the incident optical intensity and $I = 2\varepsilon_0 n_r c |\tilde{E}|^2$.

As seen in Equation (10), since the third-order nonlinear optical absorption coefficient $\frac{\Delta n^{(3)}}{n}$ is negative and is also proportional to the incident optical intensity I , the total absorption coefficient $\frac{\Delta n}{n}$ is decreases as I increases.

3. RESULTS AND DISCUSSION

We have calculated the linear, the third-order nonlinear and the total RI changes given by Equations (9)–(11) for the spherical QD, GaAs/ $\text{Al}_x\text{Ga}_{1-x}\text{As}$. We have used the material parameters of GaAs for the well region and that of $\text{Al}_x\text{Ga}_{1-x}\text{As}$ for the barrier region since their physical parameters are well known, which are given in Ref. [36] as the functions of stoichiometric ratio x , which is known Aluminium concentration ratio. The difference between the band gaps of GaAs and $\text{Al}_x\text{Ga}_{1-x}\text{As}$ is $\Delta E_g(x) = (1.155x + 0.37x^2)$ eV, the effective dielectric constant is $\varepsilon(x) = (13.18 - 3.12x)$ and the effective electron mass is $m(x) = (0.0665 + 0.0835x)m_0$, m_0 is the free-electron mass. We have used 60% of the band gap difference for the confining potential V_0 as suggested in Ref. [36]. The parameters used in our calculations are as follows: the relaxation time $\tau = 0.2$ ps, $n_r = 3.15$ and $\rho = 3 \times 10^{22} \text{ m}^{-3}$. Using the above given parameters of GaAs ($x = 0$) one can obtain the effective Bohr radius and the effective Rydberg energy as $\cong 101 \text{ \AA}$ and

$\cong 5.72$ meV, respectively. We have used the energy eigenvalues E_i and the wavefunctions ψ_i which were obtained by Özmen et al. [17].

Photoabsorption process may be defined as an optical (intersub-band) transition in low dimensional quantum mechanical systems. The photoabsorption occurs from a lower state to an upper state with absorbing a photon.

Figures 1 and 2 display the square of dipole transition matrix element between i th and f th states and differences between energy levels in the dipole transitions as a function of dot radius at $x = 0.3$. As can be seen from these figures, energy differences between the levels are large in small dot radii, whereas the square of dipole matrix elements

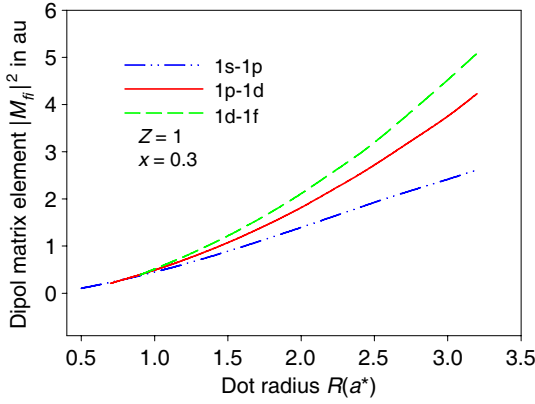


Figure 1. The variation of the square of dipole matrix element of the QD with impurity as a function of dot radius.

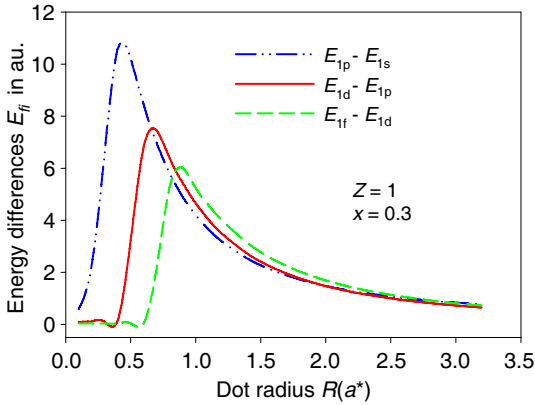


Figure 2. The variation of difference between the energy levels of the QD with impurity as a function of dot radius.

is small. On the other hand, in large dot radii, while energy differences are going to small value, the square of dipole matrix element increase quickly.

RI changes are important parameters in investigation of optical properties of QDs. In Figure 3, we plot the linear, nonlinear and total RI changes for the transitions 1s-1p, 1p-1d and 1d-1f in the QD with impurity as a function of photon energy $\hbar\omega$ at $R = 1a^*$. As seen from Figure 3, the linear RI change increases constantly with increasing photon energy until it reaches a maximum value, which happened in the normal dispersion, defined by $dn/d\omega > 0$. As the photon energy approaches the threshold energy, the sign of normal dispersion changes and the anomalous dispersion, defined by $dn/d\omega < 0$, is found in the resonance frequency of the QD. This region is known as an absorption band since photon is very strongly absorbed. While going up the transition between higher energy levels, the maximum values of RI changes move toward higher energy region because the energy differences between higher levels increase. As for the total RI, the linear change generated by the term $\chi^{(1)}$ in the RI is positive, whereas the third-order nonlinear change generated by the term $\chi^{(3)}$

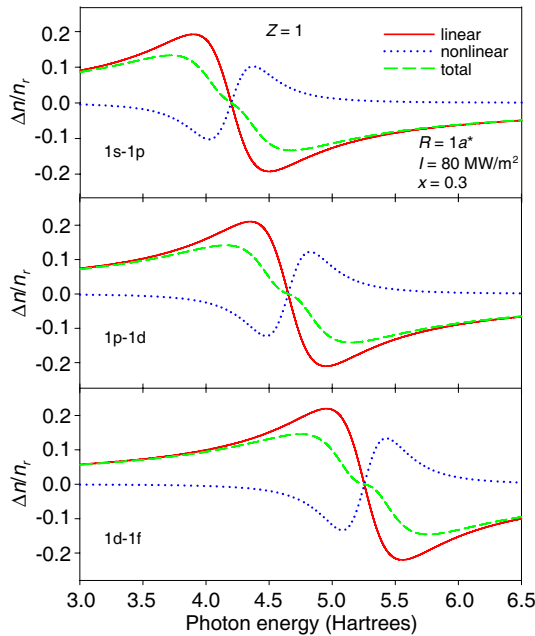


Figure 3. The linear, the nonlinear and the total RI changes for transitions 1s-1p, 1p-1d and 1d-1f in the QD with impurity as a function of incident photon energy ($\hbar\omega$).

is negative. Therefore the total RI change is significantly reduced by the nonlinear contribution. The contributions of both the linear and the third-order nonlinear RI changes should be considered especially for those operating under high incident optical intensity I .

Figure 4 shows the total RI changes of the QD for the transitions 1s-1p, 1p-1d and 1d-1f as a function of photon energy for three different values of the dot radii $R = 0.9a^*$, $1.4a^*$ and $3a^*$ for case with impurity at $I = 80 \text{ MW/m}^2$ and $x = 0.3$. As seen from Figure 4, the RI changes strongly depend on dot radius of QD. The energy difference in QD increases as dot radius decreases. Thus, the RI changes display a

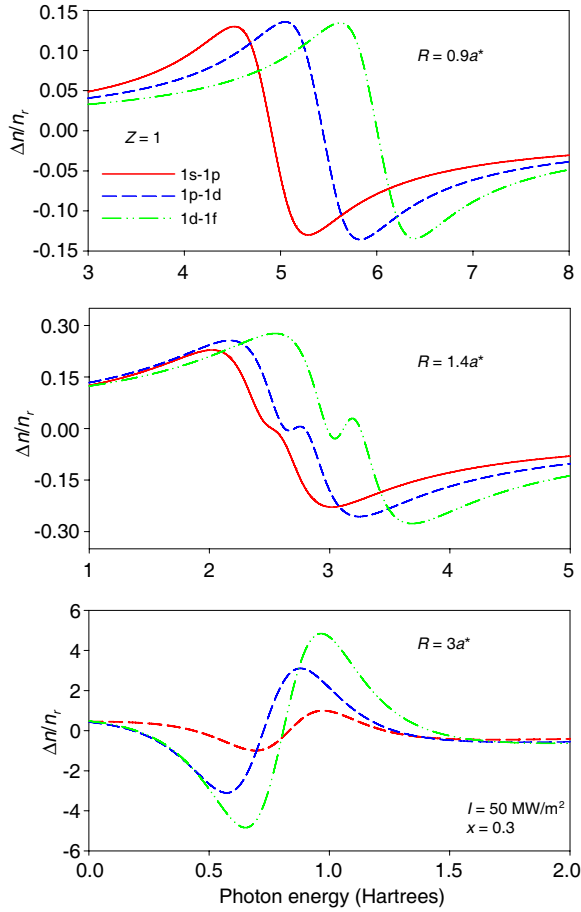
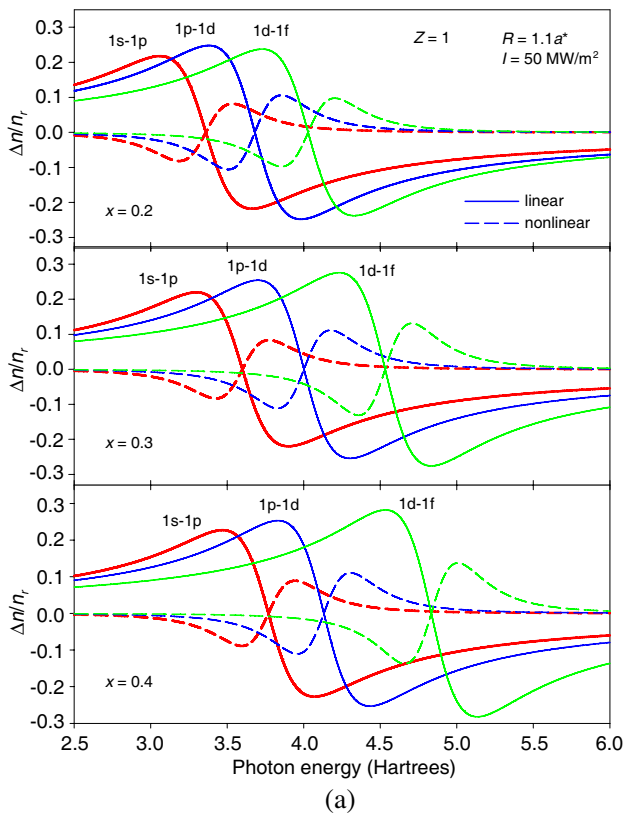


Figure 4. The total RI changes for the transitions 1s-1p, 1p-1d and 1d-1f in the QD with impurity as a function of incident photon energy $\hbar\omega$ for three different values of dot radius at $x = 0.3$.

shift toward lower energy (red shift) as the dot radius increases. All transitions are shown the same characteristic feature. As the dot radius increases, the peak values of total RI changes move toward lower energy regions. At the same time, the amplitudes of the RI changes increase as the dot radius increases. On the other hand, while the intensity of linear RI term increases in small dot radii, the intensity of nonlinear term increases in large dot radii. That is, as the linear term is more effective in small dot radii, the nonlinear term is more effective in large dot radii. The reason is that as the energy difference of the levels is more dominant in small dot radii, the dipole transition matrix element is more dominant in large dot radii, see Figure 1 and Figure 2. As a result of this case, the total RI changes turn upside-down in large dot radii.

For cases with impurity, in Figures 5(a) and (b), we display the linear and nonlinear RI changes for the transitions 1s-1p, 1p-1d and 1d-1f as a function of photon energy for three different values of the stoichiometric ratio x : 0.2, 0.3 and 0.4 for the dot radii $R = 1.1a^*$ and



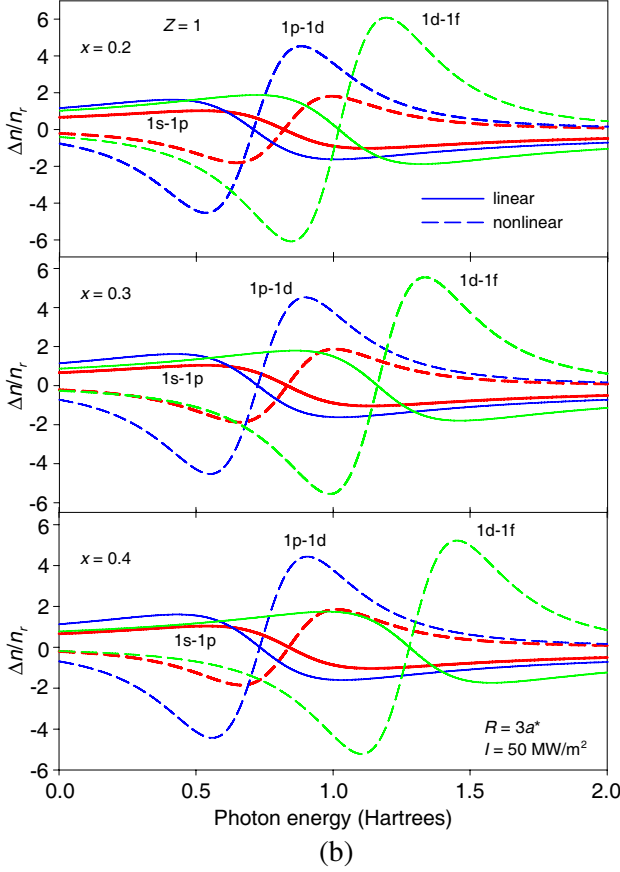


Figure 5. The linear and the nonlinear RI changes for the transitions 1s-1p, 1p-1d and 1d-1f in the QD with impurity as a function of incident photon energy ($\hbar\omega$) for three different values of the stoichiometric ratio: $x = 0.2, 0.3$ and 0.4 : (a) for the dot radius $R = 1.1a^*$ and (b) for the dot radius $R = 3a^*$.

$3a^*$. The confining potential V_0 corresponding to these stoichiometric ratios are 147.48 meV, 228 meV and 313 meV, respectively. In all transitions, the peak values and the amplitudes of the linear and the nonlinear RI changes move toward larger energy regions because the energy difference between subbands for the same dot radius increases with increasing V_0 . In addition, the amplitudes of the RI changes increase while going up the transitions between higher energy levels at the same stoichiometric ratio. This is because that the dipole matrix element of the transitions between higher energy levels increases more

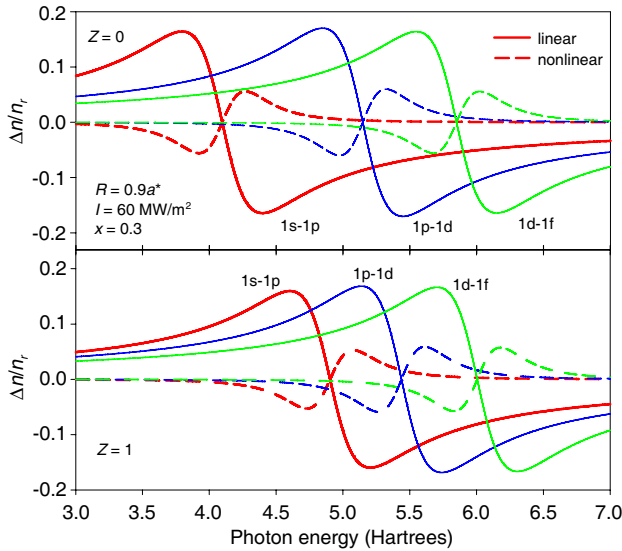


Figure 6. The linear and the nonlinear RI changes for the transitions 1s-1p, 1p-1d and 1d-1f in the QD with and without impurity as a function of the incident photon energy ($\hbar\omega$) at $R = 0.9a^*$.

than that of lower energy levels, seen Figure 1. It is clearly seen that the maximum values of the RI changes move toward higher photon energy region while increasing the stoichiometric ratio x (or confining potential), especially at strong and medium confining potential regions. On the other hand, as seen from Figure 5(b), as the dot radius increase, the nonlinear RI term is more dominant when compared with the linear RI term. In large dot radii, because the effect of confinement potential is very little, maximum values of the RI changes shift toward lower photon energy regions, redshift. However, the amplitudes of the RI changes increase in large dot radii. Also we have seen that the peak values of the RI changes in the transitions 1p-1d shift to the lower photon energy region more than that of the 1s-1p. The reason for this, the energy difference of the 1p-1d, 0.726557, is smaller than that of the 1s-1p, 0.833425, at $R = 3a^*$, as seen from Figure 2.

Understanding the effect of impurity on the electronic states of semiconductor structures is important in semiconductor physics because their presence can dramatically alter the performance of quantum devices, optical and transport properties [37]. In Figure 6, the linear and the third-order nonlinear RI changes of the QD for the transitions 1s-1p, 1p-1d and 1d-1f have illustrated as a function of the photon energy for cases with and without impurity at $x = 0.3$,

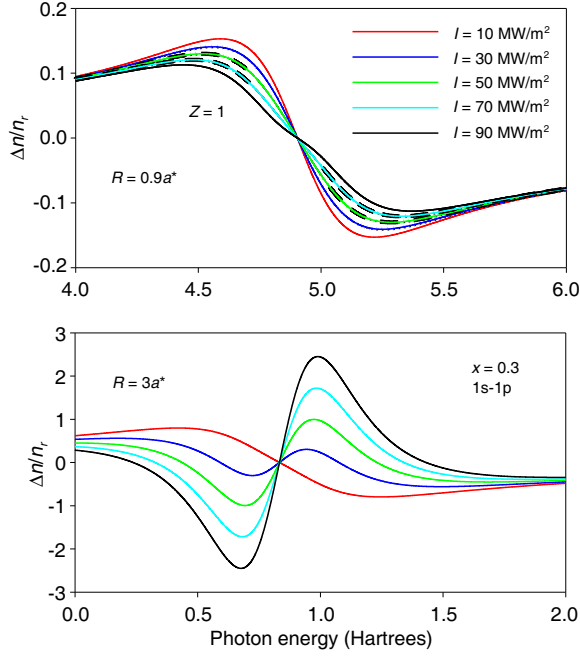


Figure 7. The total RI changes for the transitions 1s-1p in the QD with impurity as a function of incident photon energy ($\hbar\omega$) for five different values of the incident optical intensity at the dot radii $R = 0.9a^*$ and $3a^*$.

$I = 60 \text{ MW/m}^2$ and $R = 0.9a^*$. For all transitions it is obviously shown that the peaks of linear and nonlinear RI changes of the QD with impurity move toward higher photon energy region, blue shift, compared with the case without impurity. This shift is more significant in the transitions between lower energy states where electron is more localized near the impurity. Besides, it is clearly seen that presence of impurity decreases the amplitudes of the linear and the third-order nonlinear RI changes, especially in small dot radii.

The nonlinear RI term has a considerable contribution to magnetude of the RI changes. In order to illustrate this effect, we have demonstrated the total RI changes in Figure 7 as a function of the photon energy $\hbar\omega$ for five different values of the incident optical intensities $I = 10, 30, 50, 70$ and 90 MW/m^2 for the transitions 1s-1p at the dot radii $R = 0.9a^*$ and $3a^*$. As seen from the curves in Figure 7, as the incident optical intensity I increases, the total RI changes are reduced. The higher incident optical intensity I causes to increase the nonlinear RI term, but the linear RI term does not change with increasing the optical intensity I . However, these two terms are

opposite in sign, so the stronger the optical intensity is, the larger the nonlinear term will be, but the total RI changes are reduced. Therefore, a relatively weaker incident optical intensity should be employed if it is desired to obtain a larger change in the RI. There are small shifts at the peak values of the curves as the incident optical intensity I increases. On the other hand, as seen from the curves in $R = 3a^*$, the total RI changes turn upside-down in large dot radii as the optical intensity I increases, as seen in Figure 4, and the amplitudes of the total RI changes increase as the optical intensity I increases because the nonlinear term is more dominant.

4. CONCLUSION

We have investigated the RI changes for the transitions 1s-1p, 1p-1d and 1d-1f in the spherical QD, GaAs/Al_xGa_{1-x}As, with and without impurity. Impurity, stoichiometric ratio, dot radius and incident optical intensity has a great influence on the linear, nonlinear and total RI changes. Moreover, the magnitudes of the linear, nonlinear and total RI changes increase for transitions between higher energy levels. This result is in good agreement with the literature result [32]. To our knowledge there are very few reports of the absorption spectra including the transitions between higher electronic states in QDs. With respect to the lack of such studies, we believe that our study makes an important contribution to the literature. The theoretical investigation of the optical RI changes in spherical QDs will lead to a better understanding of the properties of QDs. Such theoretical studies may have profound consequences about practical application of the electro-optical devices, and the optical absorption saturation also has extensive application in the optical communication.

ACKNOWLEDGMENT

This work is partially supported by Selçuk University BAP office.

REFERENCES

1. Maksym, P. A. and T. Chakraborty, "Quantum dots in a magnetic field: Role of electron-electron interactions," *Phys. Rev. Lett.*, Vol. 65, 108, 1990.
2. Bose, C. and C. K. Sarkar, "Effect of a parabolic potential on the impurity binding energy in spherical quantum dots," *Physica B*, Vol. 253, 238, 1998.

3. Niculescu, E. C., "Energy levels in a spherical quantum dot with parabolic confinement under applied electric fields," *Mod. Phys. Lett. B*, Vol. 15, 545, 2001.
4. Mikhail, I. F. I. and I. M. M. Ismail, "Binding energy of an off-centre hydrogenic donor impurity in a spherical quantum dot," *Phys. Stat. Sol. (B)*, Vol. 244, 3647, 2007.
5. Çakır, B., A. Özmen, Ü. Atav, H. Yüksel, and Y. Yakar, "Investigation of electronic structure of a quantum dot using slater-type orbitals and quantum genetic algorithm," *Int. J. Mod. Phys. C*, Vol. 18, 61, 2007.
6. Çakır, B., A. Özmen, Ü. Atav, H. Yüksel, and Y. Yakar, "Calculation of electronic structure of a spherical quantum dot using a combination of quantum genetic algorithm and Hartree-Fock-Roothaan method," *Int. J. Mod. Phys. C*, Vol. 19, 599, 2008.
7. Aquino, N., "The hydrogen and helium atoms confined in spherical boxes," *Adv. Quantum Chem.*, Vol. 57, 123, 2009.
8. Patil, S. H. and Y. P. Varshni, "Properties of confined hydrogen and helium atoms," *Adv. Quantum Chem.*, Vol. 57, 1, 2009.
9. Sadeghi, E., "Impurity binding energy of excited states in spherical quantum dot," *Physica E*, Vol. 41, 1319, 2009.
10. Duque, C. A., E. Kasapoğlu, S. Sakiroğlu, H. Sari, and E. Sökmen, "Intense laser effects on donor impurity in a cylindrical single and vertically coupled quantum dots under combined effects of hydrostatic pressure and applied electric field," *Apply Surf. Sci.*, Vol. 256, 7406, 2010.
11. Mikhail, I. F. I. and I. M. M. Ismail, "Hydrogenic impurity in a quantum dot: Comparison between the variational and strong perturbation methods," *Superlattices Microstruct.*, Vol. 48, 388, 2010.
12. Nasri, D. and N. Sakkal, "General properties of confined hydrogenic impurities in spherical quantum dots," *Physica E*, Vol. 42, 2257, 2010.
13. Ahn, D. and S. L. Chuang, "Calculation of linear and nonlinear intersubband optical absorptions in a quantum-well model with an applied electric-field," *J. Quantum Electronics*, Vol. 23, 2196, 1987.
14. Kuhn, K. J., G. I. Iyengar, and S. Yee, "Free carrier induced changes in the absorption and refractive index for intersubband optical transitions in $\text{Al}_x\text{Ga}_{1-x}\text{As}/\text{GaAs}/\text{Al}_x\text{Ga}_{1-x}\text{As}$ quantum wells," *J. Appl. Phys.*, Vol. 70, 5010, 1991.
15. Liu, C. H. and B. R. Xu, "Theoretical study of the optical

- absorption and refraction index change in a cylindrical quantum dot,” *Phys. Lett. A*, Vol. 372, 888, 2008.
16. Wang, G., Q. Guo, and K. Guo, “Refractive index changes induced by the incident optical intensity in semiparabolic quantum wells,” *Chin. J. Phys.*, Vol. 109, 063108, 2011.
 17. Özmen, A., Y. Yakar, B. Çakır, and Ü. Atav, “Computation of the oscillator strength and absorption coefficients for the intersubband transitions of the spherical quantum dot,” *Opt. Commun.*, Vol. 282, 3999, 2009.
 18. Yakar, Y., B. Çakır, and A. Özmen, “Linear and nonlinear optical properties in spherical quantum dots,” *Commun. Theor. Phys.*, Vol. 53, 1185, 2010.
 19. Çakır, B., Y. Yakar, A. Özmen, M. Ö. Sezer, and M. Şahin, “Linear and nonlinear optical absorption coefficients and binding energy of a spherical quantum dot,” *Superlattices Microstruct.*, Vol. 47, 556, 2010.
 20. Yakar, Y., B. Çakır, and A. Özmen, “Calculation of linear and nonlinear optical absorption coefficients of a spherical quantum dot with parabolic potential,” *Opt. Commun.*, Vol. 283, 1795, 2010.
 21. Chen, B., K. X. Guo, R. Z. Wang, Z. H. Zhang, and Z. L. Liu, “Linear and nonlinear intersubband optical absorption in double triangular quantum wells,” *Solid State Commun.*, Vol. 149, 310, 2009.
 22. Bau, N. Q., L. T. Hung, and N. D. Nam, “The nonlinear absorption coefficient of a strong electromagnetic wave by confined electrons in quantum wells under the influences of confined phonons,” *Journal of Electromagnetic Waves and Applications*, Vol. 24, No. 13, 1751–1761, 2010.
 23. Trein, H. D. and N. V. Nhan, “The nonlinear absorption of a strong electromagnetic waves caused by confined electrons in a cylindrical quantum wire,” *Progress In Electromagnetics Research Letters*, Vol. 20, 87–96, 2011.
 24. Şahin, M., “Photoionization cross section and intersublevel transitions in a one- and two-electron spherical quantum dot with a hydrogenic impurity,” *Phys. Rev. B*, Vol. 77, 045317, 2008.
 25. Şahin, M., “Third-order nonlinear optical properties of a one- and two-electron spherical quantum dot with and without a hydrogenic impurity,” *J. Appl. Phys.*, Vol. 106, 063710, 2009.
 26. Yuan, J. H., J. S. Huang, M. Yin, O. J. Zeng, and J. P. Zhang, “The correlation energies and nonlinear optical absorptions of an

- exciton in a disc-like quantum dot,” *Opt. Commun.*, Vol. 283, 3529, 2010.
27. Shao, S., K. X. Guo, Z. H. Zhang, N. Li, and C. Peng, “Studies on the third-harmonic generations in cylindrical quantum dots with an applied electric field,” *Superlattices Microstruct.*, Vol. 48, 541, 2010.
 28. Rezaei, G., B. Vaseghi, F. Taghizadeh, M. R. K. Vahdani, and M. J. Karimi, “Intersubband optical absorption coefficient changes and refractive index changes in a two-dimensional quantum pseudodot system,” *Superlattices Microstruct.*, Vol. 48, 450, 2010.
 29. Zhang, L., Z. Yu, W. Yao, Y. Liu, and H. Ye, “Linear and nonlinear optical properties of strained GaN/AlN quantum dots: Effects of impurities, radii of QDs, and the incident optical intensity,” *Superlattices Microstruct.*, Vol. 48, 434, 2010.
 30. Rezaei, G., M. R. K. Vahdani, and B. Vaseghi, “Nonlinear optical properties of a hydrogenic impurity in an ellipsoidal finite potential quantum dot,” *Current Appl. Phys.*, Vol. 11, 176, 2011.
 31. Zhang, Z. H., K. X. Guo, B. Chen, R. Z. Wang, M. W. Kang, and S. Shao, “Theoretical studies on the optical absorption coefficients and refractive index changes in parabolic quantum dots in the presence of electric and magnetic fields,” *Superlattices Microstruct.*, Vol. 47, 325, 2010.
 32. Kamanina, N. V. and A. I. Plekhanov, “Mechanisms of optical limiting in fullerene-doped pi-conjugated organic structures demonstrated with polyimide and COANP molecules,” *Optics and Spectroscopy*, Vol. 93, 408, 2002.
 33. Duque, C. A., E. Kasapoğlu, S. Sakiroğlu, H. Sari, and E. Sökmen, “Intense laser effects on nonlinear optical absorption and optical rectification in single quantum wells under applied electric and magnetic field,” *Apply Surf. Sci.*, Vol. 257, 2313, 2011.
 34. Kirak, M., S. Yilmaz, M. Şahin, and M. Gençaslan, “The electric field effects on the binding energies and the nonlinear optical properties of a donor impurity in a spherical quantum dot,” *J. Appl. Phys.*, Vol. 109, 094309, 2011.
 35. Boyd, W., *Nonlinear Optics*, 2nd edition, Academic Press, New York, 2003.
 36. Adachi, S., *GaAs and Related Materials: Bulk Semiconducting and Superlattice Properties*, World Scientific, Singapore, 1994.
 37. Queisser, H. J. and E. E. Haller, “Defects in semiconductors: Some fatal, some vital,” *Science*, Vol. 281, 945, 1998.